Bioconjugate Chemistry

Article

pubs.acs.org/bc

Glycerol-Based Contrast Agents: A Novel Series of Dendronized Pentamethine Dyes

Virginia Wycisk,[†] Jutta Pauli,[‡] Pia Welker,[§] Aileen Justies,[†] Ute Resch-Genger,[‡] Rainer Haag,[†] and Kai Licha*[,§]

[†]Freie Universität Berlin, Takustr. 3, 14195 Berlin, Germany

[§]mivenion GmbH, Robert-Koch-Platz 4, D-10115 Berlin, Germany

[‡]BAM Federal Institute for Material Research and Testing, Division Biophotonics, 12489 Berlin, Germany

Supporting Information

ABSTRACT: The synthesis of water-soluble dyes, which absorb and emit in the range between 650 and 950 nm and display high extinction coefficients (ε) as well as high fluorescence quantum yields (Φ_f), is still a demand for optical imaging. We now present a synthetic route for the preparation of a new group of glycerol-substituted cyanine dyes from dendronized indole precursors that have been functionalized as *N*-hydroxysuccinimide (NHS) esters. High Φ_f values of up to 0.15 and extinction coefficients of up to 189 000 L mol^{-1} cm^{-1} were obtained for the pure dyes. Furthermore, conjugates of the new dendronized dyes with the antibody cetuximab (ctx) that were directed against the epidermal growth factor receptor (EGFR) of tumor cells could be prepared with dye to protein ratios between 0.3 and 2.2 to assess their potential as imaging probes. For the first time, ctx conjugates could be achieved without showing a decrease in Φ_f and with an increasing labeling degree that exceeded the value of the pure dye even at a labeling degree above 2. The incorporation of hydrophilically and sterically demanding dendrimers into cyanines prevented dimer formation after covalent conjugation to the antibody. The binding functionality of the resulting ctx conjugates to the EGFR was successfully demonstrated by cell microscopy studies using EGFR expressing cell lines. In summary, the combination of hydrophilic glycerol dendrons with reactive dye labels has been established for the first time and is a promising approach toward more powerful fluorescent labels with less dimerization.

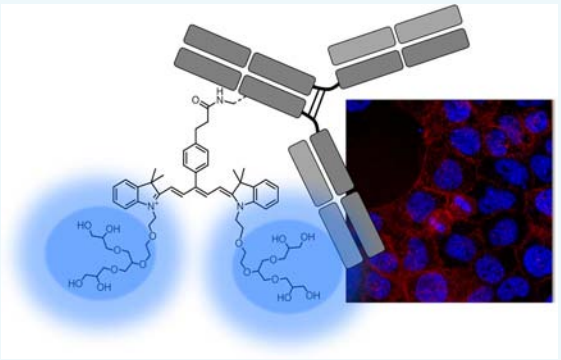

INTRODUCTION

Optical imaging technologies are crucial for drug discovery research and can be used to investigate tissue anatomy and physiology by applying nonionizing, harmless radiation and fluorescent dyes in low concentrations. A high fluorescence quantum yield, stability in biological systems, and a good solubility in preferably aqueous solvents without aggregation or precipitation are required when designing fluorescent dyes for optical imaging.[1] Many different fluorophores fulfill these conditions and are being applied for medical imaging, but most of the published work involves cyanine dyes, which have been synthesized in many ways in recent years.[2] This large group of fluorophores is characterized by a broad spectrum ranging from visible to near-infrared (NIR) absorption and fluorescence resulting in various applications, e.g., in silver halide photography,[3] as laser materials,[4−8] or as antitumor agents.[9] Modifications of side chains and aromatic substitutions create molecules with different solubilities and absorption maxima, which can be conjugated to biomolecules, so that these dyes can be used for in vivo imaging.

As observed with indocyanine green (ICG), carbocyanine dyes are generally known for their self-aggregation in solution due to intermolecular interactions between the molecules. Aggregation patterns can be noted in absorption spectra as two significant bands: J-bands, which are named after Jelly, the first investigator of these effects, and are bathochromic shifts; and H-bands, which are hypsochromic shifts.[10−12] H-aggregates, which shift to smaller wavelengths, are characterized by a parallel orientation of the dye molecules stacked plane-to-plane, while end-to-end stacks mark the J-aggregates. Generally, the introduction of chemical groups can influence the dye aggregation, especially sulfonate groups, which create electrostatic shielding,[13] or polyfluorinated cyanine dyes, which indicate reduced aggregation due to electronic effects.[14] The overall goal of these attempts to design novel fluorophores is to enhance the fluorescence quantum yields to a maximum in order to facilitate applications in imaging technologies. Beyond electrostatic and electronic effects, the third approach to minimize aggregation of fluorophores would be to exploit steric effects, which can be achieved by adding large groups,

Received: February 14, 2015
Revised: March 24, 2015
Published: March 26, 2015

DOI: 10.1021/acs.bioconjchem.5b00097
Bioconjugate Chem. 2015, 26, 773−781

preferably dendritic structures. The size of these moieties is a considerable challenge because large sizes could block the functionality of the targeting biomolecule on its surface. On the other hand, these groups have the potential to enhance the water solubility of the fluorophore. Based on a completely different fluorophore system, the perylene dyes, Haag and Zimmerman et al. demonstrated that polyglycerol dendrons can act as new promising structures to increase hydrophilicity and to prevent aggregation of perylene bisimide dyes.[15−17] For perylenes, which are not soluble in water, such dendrons were able to increase water solubility stepwise and decrease quenching depending on the dendron generation. Other fluorophores such as fluorescein can be attached to polymers, which increases photostability and the fluorescence quantum yield in relation to the free dyes.[18] Based on these results, we designed 4 different pentamethine dyes with glycerol-based substituents (see Figure 1) in order to increase the hydrophilicity and improve optical properties. The dyes were equipped with generation 1 dendrons [G1.0] with a total of 8 hydroxy functionalities and linear polyethylene glycol chains in order to comparably study whether these groups can suppress aggregation and therefore increase fluorescence quantum yields. At the conjugated chain, a meso-positioned linker with a carboxy functional group enables further reactions, e.g., bioconjugation. We present here the synthesis of fluorophores with a new substitution pattern and compare their fluorescence properties with other cyanine dyes. Microscopy studies on cellular binding and uptake have revealed the bioconjugates' functionality and qualify these novel cyanine dyes as fluorescent labels for biomedical imaging.

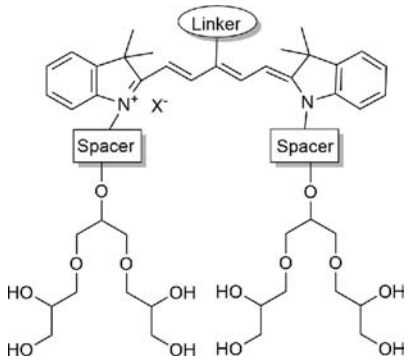

Figure 1. Illustration of a dendronized pentamethine dye.

RESULTS AND DISCUSSION

Dye Synthesis. We have synthesized different pentamethine dyes carrying sterically demanding glycerol-based side chains to minimize aggregation. In order to establish dendron moieties of a [G1.0] structure, the synthesis was started with the alkylation of acetal protected triglycerol[19,20] and yielded structures with different terminal reactive groups for further modification and subsequent coupling reactions with indolenine molecules. The alkylation was carried out using different alkene bromides and a dibromealkane shown in Scheme 1. While **2c** can be directly used for other reactions, the allylated dendrons **2a−b** were further modified by an ozonolysis reaction with subsequent mesylation to generate a leaving group. The modification was carried out according to known procedures[19,20] and yielded dendrons **4a** and **4b** with 52% and 46% yields, respectively, in all the steps.

To establish the desired synthetic approach, our focus was set on the readily available 2,3,3-trimethylindolenine. This precursor was alkylated with dendrons **2c**, **4a**, and **4b** under reflux for 1.5 days[21] and treated with hydrogen chloride in methanol overnight for acetal deprotection to get the desired indolenines **5a−c** shown in Scheme 2. For further characterization and spectroscopic comparison, a PEGylated indolenine derivative **5d** was prepared from the previously mesylated,[22] defined mPEG−OH of 11 oxyethylene units. Since a purification of the indole derivatives was not possible, the impure indoles were submitted to dye synthesis in excess and purity was roughly estimated from ^{1}H NMR (60−90%) in order to ensure an optimized dye formation.

Indole derivatives **5a−d** were condensed with bromo malondianil[23] **6** and yielded 49−86% of dyes **7a−d**.[24,25] This synthetic approach leads to structures containing bromine at the meso-position of the conjugated chain, which is useful for postsynthetic transformations, and in our case, for the introduction of a moiety with a terminal carboxyl group for bioconjugation via Suzuki coupling. The Pd-catalyzed cross coupling was carried out using 4-(2-carboxyethyl) benzenebor-

Scheme 1. Preparation of Dendron Precursors[a]

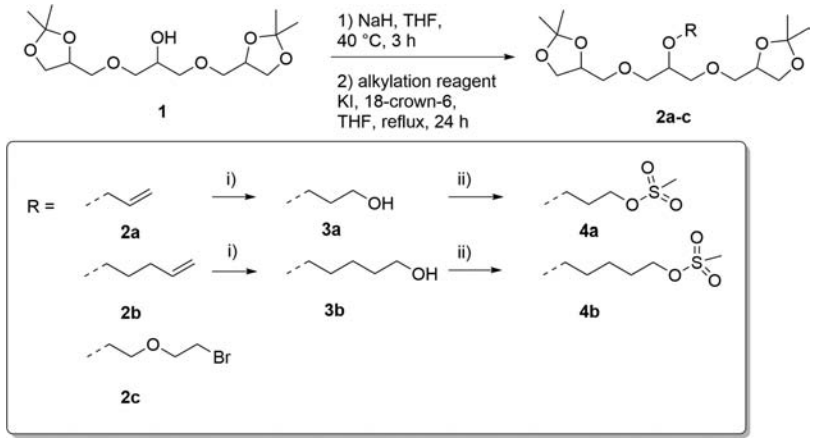

[a](i) (1) ozone, CH_2Cl_2/methanol, −78 °C, (2) O_2, CH_2Cl_2/methanol, $NaBH_4$, overnight, rt, (ii) methane sulfonyl chloride, NEt_3, toluene, 0 °C → rt, 2 h.

DOI: 10.1021/acs.bioconjchem.5b00097
Bioconjugate Chem. 2015, 26, 773−781

Scheme 2. Synthesis of Glycerol-Modified Dyes Starting from Indolenine Precursors

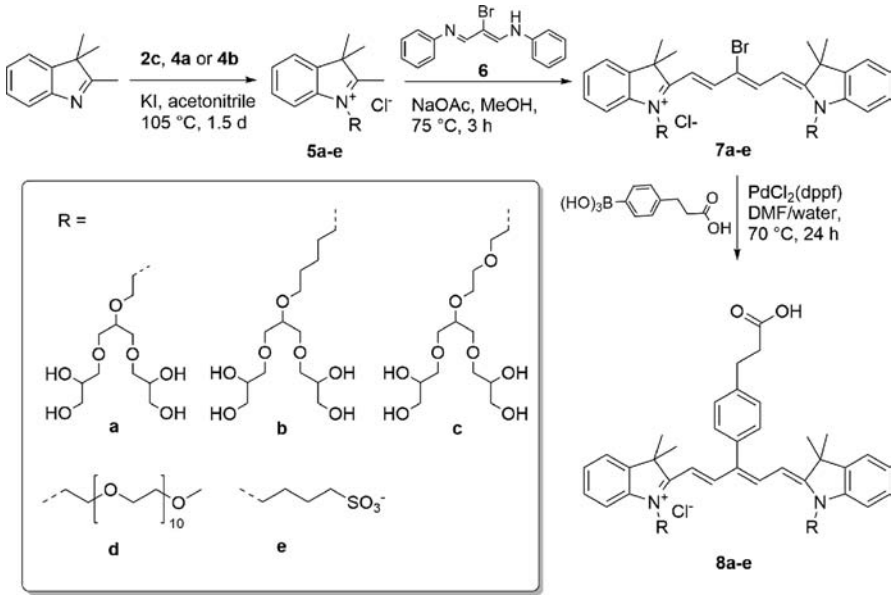

Table 1. Optical Properties of the Examined Free Dyes 8a−e

dye	solvent	λ_{abs}, nm	λ_{em}, nm	Stokes shift, nm	ε, L mol^{-1}·cm^{-1}	Φ_f	B
8a	PBS	643	667	24	87000	0.12	11000
	PBS/BSA	644	668	24	92000	0.14	13000
8b	PBS	644	668	24	189000	0.15	29000
	PBS/BSA	646	673	27	190000	0.27	52000
8c	PBS	643	666	23	107000	0.12	13000
	PBS/BSA	644	667	23	112000	0.14	16000
8d	PBS	643	666	23	169000	0.13	22000
	PBS/BSA	644	668	24	*n.d.*	0.16	*n.d.*
8e	PBS	643	665	22	192000	0.09	18000
	PBS/BSA	658	678	20	135000	0.45	61000

onic acid (deprotonated) and yielded 31−74% of dyes **8a−e**.[26] Conversion into NHS esters using HSTU yielded active esters **9a−e** for conjugation with biomolecules, with the antibody cetuximab (ctx) targeting the epidermal growth factor receptor of the tumor cells. Purification was done on a Sephadex column in order to separate the desired conjugate from the excess free dye, which yielded conjugates **10b−e** with different D/Ps for spectroscopic characterization.

Spectroscopic Properties of the Free Dyes. For spectroscopic characterization, we determined and compared molar absorption coefficients and fluorescence quantum yields in PBS and 5% (w/w) BSA (PBS/BSA) modeling body fluid of the free carboxy dyes **8a−d** along with dye **8e**, which had a common substitution pattern of sulfobutyl chains, as widely established in commercial cyanine dyes. The results are summarized in Table 1. While dyes **8b** and **8d** showed molar absorption coefficients similar to the reference dye **8e**, two of the dendronized dyes **8a** and **8c** revealed rather small coefficients of around 100 000 L·mol^{-1} cm^{-1}. The different values can be correlated with the structural nature of the side chain. Hence, the existence of oxygen as a heteroatom within the alkyl chain in combination with the dendron moieties might lead to the decrease of the absorption coefficients, as dye **8b** with a purely aliphatic five-carbon chain exhibits an ε value that is similarly high as the reference dye. In contrast, the long PEG chain in dye **8d**, with oxygen in the same position, does not hamper the absorption coefficient. Compared to PBS solution, dendronized dyes **8a−d** show slightly enhanced extinction coefficients in 5% BSA solution in contrast to **8e**, which exhibits less ε in PBS/BSA as well as a redshift of the absorption maximum of 15 nm, which is typical for a strong protein interaction. We assume that the chosen glycerol substituents suppress the protein interaction due to a steric effect. This effect is well-known for polyglycerols and has been a research rationale for novel types of protein-resistant surfaces.[20,27]

With fluorescence quantum yields Φ_f around 0.12 and 0.15, the new dyes show comparable Φ_f values in PBS and exceed the Φ_f value of the reference dye **8e**. While the Φ_f values remained constant in PBS and PBS/BSA solution for the majority of the glycerol-based dyes, the Φ_f values increased for dyes **8b** and **8e** most likely due to protein−dye interactions. Again, the existence of oxygen as a heteroatom might be employed to explain that dyes **8a**, **8c**, and **8d** exhibit reduced protein−dye interactions and therefore lead to increased quantum efficiency. For further characterization, the brightness B was determined from the molar absorption coefficient at the dyes' absorption maximum λ_{max} and the fluorescence quantum yield ($B = \varepsilon(\lambda_{max}) \times \Phi f$). Whereas dendronized dyes in general revealed rather low values, the value of dye **8b** exceeded the one of reference dye **8e** in PBS. Due to dye−protein interactions occurring for dye **8b** and **8e** in PBS/BSA solutions, the brightness exhibited the highest value. Nevertheless, the dendronized dye **8b** clearly

DOI: 10.1021/acs.bioconjchem.5b00097
Bioconjugate Chem. 2015, 26, 773−781

had better spectroscopic properties than the reference dye **8e** with anionic side chains when neglecting the enhancing effect of protein interactions.

Optical Properties of the Conjugates. The purpose of the final part of the synthetic work was to determine the suitability of the new dyes as fluorescent labels for biomolecules. Considering the different structural characteristics and the resulting spectroscopic properties, dyes **8b−d** and reference dye **8e** were used for conjugation to antibody cetuximab with prior conversion into the corresponding NHS ester **9b−e**. Due to the increase of aggregation rates in certain environments on biomolecule surfaces, which has been described, e.g., by Pauli et al.,[28] antibody conjugates **10b−e** were prepared with different dye-to-protein ratios (D/P) that ranged from 0.3 to 2 using NHS ester dyes **9b−e** in order to investigate the influence of the D/P on aggregation tendencies.

The spectroscopic properties of ctx conjugates **10b−e** summarized in Table 2 were obtained from absorption and fluorescence spectra. Comparing the fluorescence quantum yields of the conjugates revealed a decrease of Φ_f with increased D/P for nearly all dyes examined here with the exception of **10c**, which exhibited constant Φ_f values. For the first time, the fluorescence quantum yield of a dye−conjugate did not decrease with the increasing D/P ratio. Moreover, Φ_f of the new dye conjugates **10b−d** exceeded those of **10e**, even at higher D/P, indicating that less aggregation and fluorescence quenching occurred. It is remarkable that antibodies labeled with **9b** and **9e** revealed smaller Φ_f than the other derivatives. These two dyes have in common that the substituents bear longer alkyl chains of 4 and 5 carbon atoms, whereas the dyes **8c** and **8d** have an oxygen atom in the chain, thereby introducing a PEG-like character. Comparing Φ_f of the conjugates with those of the free dyes (see Figure 2), it can be noted that **8b** and **8e** revealed smaller Φ_f values when conjugated to ctx, whereas those of **8c** and **8d** even increased upon conjugation.

The decrease in the fluorescence quantum yield with the increasing degree of labeling was mainly due to the formation of nonfluorescent dye dimers after covalent attachment of the dye to the antibody. Such dimers can be easily detected in the absorption spectra of the conjugates by a characteristic, usually shorter, wavelength shifted band. In order to obtain a better understanding of the aggregation and quenching behavior of the derivatives with different D/P ratios, we compared the excitation and absorption spectra. Excitation spectra are generated when the excitation wavelength is varied and the fluorescence intensity is measured at a constant emission wavelength. Since the excitation spectrum only shows the absorption of the fluorescent species, the comparison of the absorption and excitation spectra reveals the extent of formed dye dimers. First, spectra of the free dyes were recorded, which, as expected, did not show any differences between excitation and absorption spectra (data not shown). In contrast, comparison of the respective spectra of conjugates revealed dimerization of the dyes. We studied and compared the excitation spectra for the conjugates of the reference dye **10e** (Figure 3A) and dendronized dye **10c** (Figure 3B), which we chose as the most promising dendronized fluorophore due to the pronounced enhancement of the quantum yield upon conjugation. This comparison revealed an increase in the dimer formation for the reference dye conjugate **10e** that was already apparent at low D/P of 1. In contrast, **10c** yielded a nearly similar absorption and excitation spectrum even at higher D/P of 1.8, which is shown in Figure 3. Thus, dimer formation is suppressed in the case of **10c**, which is due to the sterically demanding dendron as well as the oxygen-containing linker of dye **8c**. The lack of dimer formation is in accordance with constant fluorescence quantum yields at different D/P ratios as described above.

Table 2. Optical Properties of the Cetuximab Dye Conjugates 10b−e

dye	D/P	λ_{abs}, nm	λ_{em}, nm	Stokes shift, nm	Φ_f
10b	0.3	648	669	21	0.12
10b	0.4	648	668	20	0.11
10b	0.5	649	668	20	0.08
10b	1.1	648	668	20	0.07
10b	1.3	648	669	21	0.07
10c	0.4	646	665	19	0.14
10c	0.7	646	666	20	0.13
10c	0.8	646	666	20	0.13
10c	1.8	648	669	21	0.15
10d	0.5	647	667	20	0.23
10d	0.7	647	665	18	0.22
10d	1.2	647	666	19	0.19
10d	2.2	647	666	19	0.12
10e	0.7	647	669	22	0.06
10e	0.9	647	668	21	0.05
10e	1.0	647	668	21	0.04
10e	2.0	646	665	19	0.03

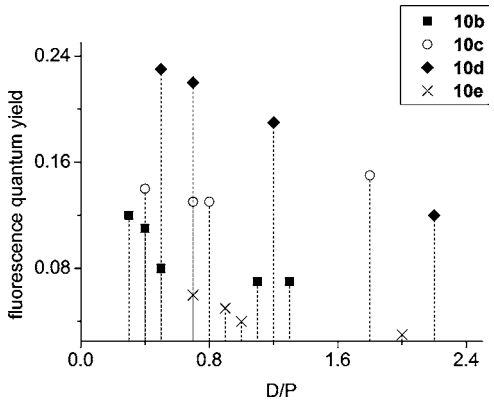

Figure 2. Quantum yields of dye cetuximab conjugates **10b−e** at different D/Ps.

Biological Characterization. The cell binding studies shown in Figure 4 were performed with a confocal fluorescence microscopy using EGFR expressing cells A431 and A549. These two cell lines were best for a qualitative exploration of the binding functionality of the EGF receptor-binding cetuximab, because A431 is known to exhibit strong expression of EGFR, whereas A549 cells express this receptor in much lower amounts on their cellular membrane. For both cetuximab conjugates labeled with **9c** and **9e**, a specific binding to the EGFR could indeed be observed for the A431 cells in fluorescence microscopy images, in which a substantial signal attributed to the cellular membrane could be clearly visualized. The negative control A549 cells did not reveal any binding to the EGFR because no signal from the studied dye was found. Thus, the novel dye conjugates based on glycerol-modified cyanine dyes are suitable fluorescence labels as demonstrated for cetuximab, which maintained its receptor binding

DOI: 10.1021/acs.bioconjchem.5b00097
Bioconjugate Chem. 2015, 26, 773−781

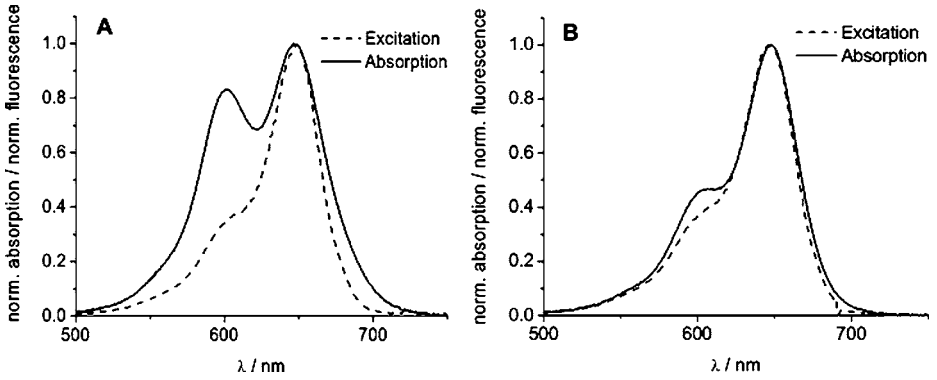

Figure 3. Excitation and absorption spectra of cetuximab conjugates **10e** (D/P = 1, A) and **10c** (D/P = 1.8, B).

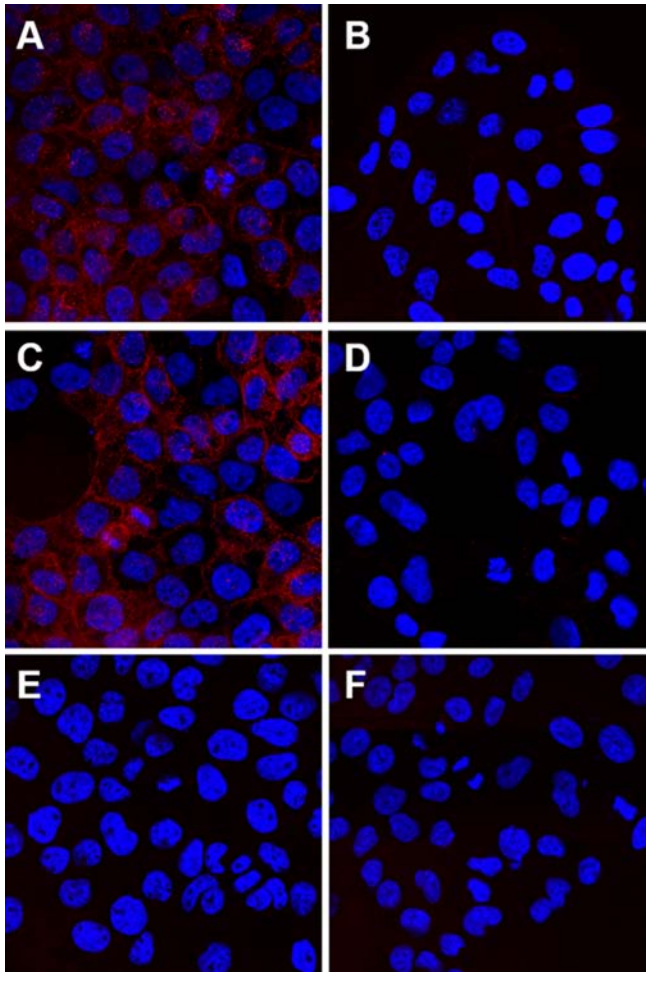

Figure 4. Fluorescence images of the cells A431 (A, C, E) and A549 (B, D, F) incubated for 1 h with cetuximab conjugates **10e** (A, B), **10c** (C, D). (E) and (F) are control measurements of the cells with a nonbinding IgG antibody.

functionality in cell culture. The reference dye with classical sulfobutyl substitution showed similar binding patterns.

CONCLUSION AND OUTLOOK

We successfully established a new route to reactive cyanine dyes employing two triglycerol units or a linear PEG chain together with a NHS ester functional group. Even without any charged side chains, the new dyes demonstrated good water solubility and are rather hydrophilic due to 8 hydroxy groups per dye molecule. Conjugation to EGFR binding antibody cetuximab via NHS ester was successfully achieved and yielded different D/Ps. The spectral characterization revealed the novel systems' advantages, because they tended to form aggregates less than analogs with sulfobutyl residues instead of triglycerol dendrons or PEG chains, especially when a full alkyl chain without its PEG-like interruption with an oxygen function could be avoided. The dendronized dyes as well as the PEG analog revealed improved spectroscopic properties including constant and solvent-independent extinction coefficients. Compared to the sulfonated reference dye, the newly synthesized cyanine dyes exhibit increased Φ_f values of up to 0.15 in the bioconjugated format. The biological characterization revealed the new dyes' ability to maintain the functionality of a receptor-binding antibody. The effects reported here should be even more pronounced for fluorophores with a higher aggregation tendency, such as indotricarbocyanines or entirely other structural types. Another effect to consider is the dendrimer size. We have confined the work to the triglycerol system, which was coupled twice to the fluorophore. Whether or not higher generations would improve optical properties remains to be studied. In conclusion, the combination of hydrophilic dendrimers, here based on glycerol, with cyanine dyes leads to fluorescent biolabels with improved properties that avoid the negatively charged side chains.

EXPERIMENTAL PROCEDURES

Synthesis. ^{1}H NMR spectra were measured on a JEOL ECX 400 spectrometer (400 MHz) and mass spectra were obtained via electrospray on an Agilent 6210 ESI-TOF spectrometer. Solvents and chemicals were commercially purchased from Sigma-Aldrich and used as received unless otherwise stated. Ethyl acetate, dichloromethane, and acetone were freshly distilled before use. Erbitux (antibody cetuximab) was purchased from Merck. Water-soluble dyes were dried on a Virtis Benchtop K 20K XL and weights of the samples were taken on a Precisa XB120A. Thin-layer chromatography (TLC) was performed on silica coated aluminum sheets using silica gel 60 F_{254} or silica gel 60 RP-18 $F_{254}S$ for reversed phase analysis. The reference dye **8e** (carboxylic acid) and 2-bromo malondianil **6** were provided by mivenion GmbH. Synthesized carbocyanine dyes were purified by reversed phase chromatography using LiChroprep RP-C18 material (40−63 μm) from Merck and a medium pressure liquid chromatography (MPLC) pump. Purification was also done by automated flash chromatography on a Combi Flash R_f (Teledyne ISCO) on normal (silica gel, 30 μm) and reversed phase material (C-18).

DOI: 10.1021/acs.bioconjchem.5b00097
Bioconjugate Chem. 2015, 26, 773−781

The purification of biomolecule conjugates was conducted on Sephadex column (NAP-25, Sephadex G-25 DNA) using PBS as solvent. Separation by centrifugation was done on a Universal 32 from Hettich and sensitive substances were shaken in a Bioshaker Q. The UV/vis spectra were recorded on a PerkinElmer LAMBDA 950 UV/vis/NIR spectrometer using disposable cuvettes from Brand. Samples for absorption measurements were dissolved in Millipore water or PBS solution (3 mM KCl, 140 mM NaCl, 0.01 M $Na_2HPO_4 \cdot 7H_2O$ in 500 mL distilled water).

Spectral Characterization. Solvents used for sample preparation were commercially purchased and used as received unless otherwise stated. Weights of samples were taken on a Sartorius supermicro S4 scale. Absorption measurements were done on a Cary 5000 spectrometer from Varian using 1 cm quartz cells, and the fluorescence measuring was performed on a FSP 920 spectrometer from Edinburgh instruments. Excitation spectra were measured on an 8100 fluorometer from SLM AMINCO. The quantum yields were determined from fluorescence emission spectra excited at 603 nm (short wavelength shoulder of absorption spectra). The dyes were measured along with the standard Oxazin 1 in order to calculate the relative quantum yields and to compare the line shape and absorption maxima.

Synthesis of Dye Labels. *Synthesis of Dendron Precursors* ***2***. NaH (3.75 g, 94 mmol, 60% dispersion in mineral oil) was added to a solution of dendron **1** (6 g, 18.73 mmol) in THF (75 mL).[20] After stirring at 40 °C for 3 h, KI (0.311 g, 1.87 mmol), 18-crown-6 (0.495 g, 1.87 mmol), and the alkylation reagent (2−20 equiv) were added to the mixture. The solution was stirred for 24 h and concentrated. The residue was extracted with CH_2Cl_2 and the combined organic phases were washed with water and saturated NaCl solution. After drying with Na_2SO_4, the crude mixture was purified by automated flash chromatography using cyclohexane/ethyl acetate (0−30% ethyl acetate). Dendron **1** (6 g, 18.73 mmol) was reacted according to the above-described procedure using 3-bromoprop-1-ene (3.4 mL, 37.5 mmol) which afforded 6.17 g (91%) of derivative **2a**. ^{1}H NMR (400 MHz, $CDCl_3$): δ 1.35 (s, 6H, CH_3), 1.41 (s, 6H, CH_3), 3.46−3.77 (m, 9H, CH_2), 3.98−4.06 (m, 2H, CH_2), 4.11−4.14 (m, 2H, CH_2), 4.22−4.28 (m, 2H, CH), 5.14−5.19 (m, 1H, $C\underline{H}_2$=CH), 5.24−5.30 (m, 1H, $C\underline{H}_2$=CH), 5.83−5.95 (m, 1H, CH_2=C$\underline{H}$); MS *m*/*z* 383.2025 ($C_{18}H_{32}O_7$ + Na^+ calculated 383.2040). Dendron **1** (200 mg, 0.62 mmol) was reacted according to the above-described procedure using 6-bromohex-1-ene (1.7 mL, 12.48 mmol) and yielded 170 mg (68%) of dendron **2b**. ^{1}H NMR (400 MHz, $CDCl_3$): δ 0.72−0.93 (m, 2H, CH_2), 1.35 (s, 6H, CH_3), 1.41 (s, 6H, CH_3), 1.53−1.62 (m, 2H, CH_2), 2.06 (q, 2H, CH_2), 3.41−3.61 (m, 12H, CH_2), 4.04 (dd, *J* = 5.6 Hz, *J* = 6 Hz, 2H, CH_2), 4.22−4.28 (m, 2H, CH), 4.93−4.95 (d, *J* = 10.4 Hz, 1H, $C\underline{H}_2$=CH), 4.98−5.02 (d, *J* = 17.2 Hz, 1H, $C\underline{H}_2$=CH), 5.74−5.85 (m, 1H, CH_2=C$\underline{H}$); MS *m*/*z* 425.2555 ($C_{21}H_{38}O_7$ + Na^+ calculated 425.2518). Dendron **1** (989 mg, 3.09 mmol) was reacted according to above-described procedure using 1-bromo-2-(2-bromoethoxy)ethane (3.9 mL, 30.09 mmol) to obtain 626 mg (43%) of dendron **2c**. ^{1}H NMR (400 MHz, $CDCl_3$): δ 1.34 (s, 6H, CH_3), 1.40 (s, 6H, CH_3), 3.43−3.81 (m, 19H, CH_2), 4.03 (m, 2H, CH_2), 4.24 (m, 2H, CH); MS *m*/*z* 493.1422 ($C_{19}H_{35}BrO_8$ + Na^+ calculated 493.1415).

Ozone was added at −78 °C to a solution of dendron **2a** or **2b** (1.62 mmol) in dry CH_2Cl_2 (11 mL) and dry methanol (14 mL) until the mixture turned blue; subsequently oxygen was added until the solution was colorless. $NaBH_4$ (16.2 mmol) was added and the mixture was stirred overnight.[20] After quenching with saturated NH_4Cl solution, the mixture was extracted with CH_2Cl_2. The combined organic layers were dried over Na_2SO_4 and the residue was purified by automated flash chromatography using cyclohexane/ethyl acetate (0−50% ethyl acetate). Dendron **2a** (584 mg, 1.62 mmol) was reacted according to the procedure described above affording compound **3a** (429 mg, 73%). ^{1}H NMR (400 MHz, $CDCl_3$): δ 1.33 (s, 6H, CH_3), 1.39 (s, 6H, CH_3), 3.21 (m, 1H, CH), 3.44−3.76 (m, 14H, CH_2), 4.02 (m, 2H, CH_2), 4.24 (m, 2H, CH); MS *m*/*z* 387.1986 ($C_{17}H_{32}O_8$ + Na^+ calculated 387.1997). Dendron **2b** (1.53 g, 3.8 mmol) was reacted according to above-described procedure to get product **3b** (0.98 g, 64%). ^{1}H NMR (400 MHz, $CDCl_3$): δ 1.35 (s, 6H, CH_3), 1.41 (s, 6H, CH_3), 1.54−1.78 (m, 6H, CH_2), 3.42−3.64 (m, 13H, CH_2), 3.73 (m, 2H, CH_2), 4.04 (m, 2H, CH_2), 4.24 (m, 2H, CH); MS *m*/*z* 429.2525 ($C_{20}H_{38}O_8$ + Na^+ calculated 429.2467).

Synthesis of Mesylates ***4***. Methane sulfonyl chloride (0.82 mmol) at 0 °C was added to a solution of dendron **3a** or **3b** (0.63 mmol) and NEt_3 (0.82 mmol) in toluene (2 mL). The mixture was stirred at 0 °C for 15 min and 2 h at rt.[19] After filtering and concentrating, the solution afforded the crude product **4a** or **4b**. Dendron **3a** (229 mg, 0.63 mmol) was reacted according to the procedure described above to obtain product **4a** (218 mg, 78%). ^{1}H NMR (400 MHz, $CDCl_3$): δ 1.33 (s, 6H, CH_3), 1.39 (s, 6H, CH_3), 3.04 (s, 3H, S-CH_3), 3.44−3.74 (m, 12H, CH_2), 3.87 (m, 1H, CH), 4.02 (m, 2H, CH_2), 4.23 (m, 2H, CH), 4.33 (m, 2H, CH_2); MS *m*/*z* 465.1774 ($C_{18}H_{34}O_{10}S$ + Na^+ calculated 465.1773). Dendron **3b** (500 mg, 1.23 mmol) was reacted according to the above-described procedure to get compound **4b** (593 mg, 100%). ^{1}H NMR (400 MHz, $CDCl_3$): δ 1.35 (s, 6H, CH_3), 1.40 (s, 6H, CH_3), 1.46 (m, 2H, CH_2), 1.59 (m, 2H, CH_2), 1.76 (m, 2H, CH_2), 2.99 (s, 3H, $SO_3C\underline{H}_3$), 3.41−3.77 (m, 13H, CH_2), 4.03 (m, 2H, CH_2), 4.22 (m, 4H, CH_2); MS *m*/*z* 507.2239 ($C_{21}H_{40}O_{10}S$ + Na^+ calculated 507.2242).

Synthesis of Trimethylindolenine Precursors ***5***. 2,3,3-Trimethylindolenine (0.23 mmol) was added to a solution of dendron **4a** or **4b** (0.23 mmol) and potassium iodide (0.02 mmol) in acetonitrile (1 mL). The mixture was stirred at 105 °C for 1.5 d and concentrated under reduced pressure. The residue was treated with HCL in methanol overnight and precipitated in diethyl ether. Dendron **4a** (100 mg, 0.23 mmol) was reacted according to the above-described procedure which gave indolenine derivative **5a** (45.1 mg, 38%). ^{1}H NMR (400 MHz, MeOD-d_4): δ 1.60 (s, 6H, CH_3), 2.68 (s, 3H, CH_3), 3.34−3.77 (m, 17H, CH_2), 4.10−4.15 (t, 2H, CH), 7.61−7.66 (m, 2H, CH_{ar}), 7.73−7.92 (m, 1H, CH_{ar}), 7.83−7.88 (m, 1H, CH_{ar}); MS *m*/*z* 426.2630 ($C_{22}H_{36}NO_7^+$ calculated 426.2486). Dendron **4b** (300 mg, 0.62 mmol) was reacted according to the above-described procedure and afforded compound **5b** (229.3 mg, 86%). ^{1}H NMR (400 MHz, MeOD-d_4): δ 1.56−1.60 (m, 2H, CH_2), 1.61 (s, 6H, CH_3), 1.65−1.71 (m, 2H, CH_2), 2.00−2.06 (m, 2H, CH_2), 2.70 (s, 3H, CH_3), 3.43−3.78 (m, 17H, CH_2), 4.51−4.54 (t, 2H, CH_2), 7.64−7.69 (m, 2H, CH_{ar}), 7.88−7.92 (m, 1H, CH_{ar}), 7.76−7.80 (m, 1H, CH_{ar}); MS *m*/*z* 468.2898 ($C_{25}H_{42}NO_7^+$ calculated 468.2956). Dendron **4c** (609 mg, 1.291 mmol) was reacted according to the procedure described above to obtain product **5c** (204 mg, 37%). ^{1}H NMR (400 MHz, MeOD-d_4): δ 1.61 (s, 6H, CH_3), 2,83 (s, 3H, CH_3), 3.37−3.77 (m, 21H, CH_2), 3.99 (t, 2H, CH_2), 7.62−7.65 (m,

DOI: 10.1021/acs.bioconjchem.5b00097
Bioconjugate Chem. 2015, 26, 773−781

2H, CH_{ar}), 7.76−7.77 (m, 1H, CH_{ar}), 7.87−7.89 (m, 1H, CH_{ar}); MS *m/z* 470.2772 ($C_{24}H_{40}NO_8^+$ calculated 470.2748). A mixture of PEG mesylate (2.38 g, 4.01 mmol)[22] and 2,3,3-trimethylindolenine (0.491 g, 3.08 mmol) in 1,2-dichlorobenzene (4 mL) was stirred at 120 °C for 2 d and concentrated under reduced pressure. 0.93 g (30%) of **5d** was obtained by purifying the residue with automated flash chromatography using dichlormethane/methanol (0−30% methanol). ^{1}H NMR (400 MHz, $CDCl_3$): δ 1.57 (s, 6H, CH_3), 2.93 (s, 3H, CH_3), 3.35 (s, 3H, CH_3), 3.43−3.64 (m, 42H, CH_2), 3.98 (t, 2H, CH), 7.48−7.57 (m, 3H, CH_{ar}), 7.76 (dd, *J* = 4 Hz, *J* = 8 Hz, 1H, CH_{ar}); MS *m/z* 658.4168 ($C_{34}H_{60}NO_{11}^+$ calculated 658.4161).

Synthesis of Pentamethine Dyes ***7*** *and* ***8***. A mixture of indolenine **5** (0.23 mmol), 2-bromomalodianil **6** (0.1 mmol), and sodium acetate (0.4 mmol) in methanol (1 mL) was heated and stirred at 75 °C for 3 h.[24−26] The dye was precipitated in diethyl ether and the residue was purified by RP-C18 column chromatography using water/methanol (0−80% methanol). Indole **5a** (30.1 mg, 0.1 mmol) was reacted according to the procedure described above to afford 71.7 mg (72%) of dye **7a** as a blue solid. ^{1}H NMR (400 MHz, MeOD-d_4): δ 1.73 (s, 12H, CH_3), 3.28−3.65 (m, 28H, CH_2), 3.89 (m, 2H, CH_2), 4.06 (m, 4H, CH_2), 4.35 (m, 4H, CH), 6.58−6.62 (dd, *J* = 12.8 Hz, *J* = 4 Hz, 2H, CH), 7.27 (m, 2H, CH_{ar}), 7.38 (m, 4H, CH_{ar}), 7.49 (d, *J* = 7.2 Hz, 2H, CH_{ar}), 8.22−8.37 (dd, *J* = 13.2 Hz, *J* = 4.4 Hz 2H, CH); MS *m/z* 965.3944 ($C_{47}H_{70}BrN_2O_{14}^+$ calculated 965.4005). Indole **5b** (204.4 mg, 0.36 mmol) was reacted according to the procedure described above and produced mg (147.3 mg, 86%) of dye **7b** as a blue solid. ^{1}H NMR (δ/ppm, MeOD-d_4, 400 MHz): δ 1.53−1.61 (m, 4H, CH_2), 1.65−1.72 (m, 4 H, CH_2), 1.77 (s, 12H, CH_3), 1.88−1.96 (m, 4H, CH_2), 3.42−3.76 (m, 4H, CH_2), 4.22 (t, *J* = 8 Hz, 4H, CH_2), 6.52 (m, *J* = 16 Hz, 2H, CH), 7.34 (t, *J* = 8 Hz, 2H, CH_{ar}), 7.40−7.49 (m, 4H, CH_{ar}), 7.55 (d, *J* = 8 Hz, 2H, CH), 8.41 (d, *J* = 16 Hz, 2H, CH); MS *m/z* 1049.4958 ($C_{53}H_{82}BrN_2O_{14}^+$ calculated 1049.4944). Indole **5c** (23.4 mg, 0.04 mmol) was reacted according to the procedure described above which produced 12.1 mg (49%) of dye **7c** as a blue solid. ^{1}H NMR (D_2O, 400 MHz): δ 1.49 (s, 12H, CH_3), 3.20−3.69 (m, 32H, CH_2), 3.80 (m, 4H, CH_2), 4.25 (m, 2H, CH), 6.36 (m, 2H, CH), 7.20 (m, 4H, CH_{ar}), 7.37 (m, 2H, CH_{ar}), 7.93 (m, 2H, CH), 7.95 (d, 2H, CH); MS *m/z* 1053.4432 ($C_{51}H_{78}BrN_2O_{16}^+$ calculated 1053.4529). A solution of indole **5d** (0.93 g, 1.2 mmol), 2-bromomalodianil (0.15 g, 0.5 mmol), and sodium acetate (0.26 g, 3.2 mmol) in acetic anhydride (2 mL) was heated and stirred at 120 °C for 45 min. The mixture was concentrated and the residue was purified by automated flash chromatography using CH_2Cl_2/methanol (0−20% methanol) and RP-C18 column chromatography using water/methanol (0−50 methanol) and afforded 0.22 g (31%) of **7d** a blue solid. ^{1}H NMR (400 MHz, MeOD-d_4): δ 1.77 (s, 12H, CH_3), 3.50−3.74 (m, 45H, CH_2, CH_3), 3.95 (t, 4H, CH_2), 4.42 (t, 4H, CH_2), 6.64 (d, *J* = 13.6 Hz, 2H, CH_{ar}), 7.34 (t, *J* =7.2 Hz, 2H, CH_{ar}), 7.42−7.47 (m, 4H, CH_{ar}), 7.55 (d, *J* = 7.6 Hz, 2H, CH_{ar}), 8.4 (d, *J* = 13.6 Hz, 2H, CH_{ar}); MS *m/z* 1429.7507 ($C_{71}H_{118}BrN_2O_{22}^+$ calculated 1429.7354). A mixture of dye **7** (20 μmol), 4-(2-carboxyethyl) benzeneboronic acid (36 μmol), and $PdCl_2$ (dppf) (3 μmol) was dissolved in DMF/water (1.7:1, 664 μL, dye concentration: 37.7 mg/mL) and was stirred at 70 °C for 24 h.[26] The mixture was centrifuged and the residue was washed with water; this procedure was repeated several times. The precipitate was evaporated and dissolved in methanol. The residue was precipitated again in diethyl ether and the precipitate was purified by RP-C18 column chromatography using water/methanol (0−80% methanol), which made dye **8**. Dye **7a** (25 mg, 20 μmol) was reacted according to the procedure described above and yielded 15.8 mg (74%) of dye **8a**. ^{1}H NMR (400 MHz, MeOD-d_6): δ 1.75 (s, 12H, CH_3), 2.51 (m, 2H, CH_2), 2.99 (m, 2H, CH_2), 3.40−3.83 (m, 34H, CH_2), 4.02 (t, 4H, *J* = 4 Hz, CH), 5.87 (d, *J* = 14 Hz, 2H, CH), 7.18−7.25 (m, 6H, CH_{ar}), 7.33 (t, *J* = 7.6 Hz, 2H, CH_{ar}), 7.44 (d, 4H, *J* = 7.6 Hz, 4H, CH_{ar}), 8.26 (d, *J* = 13.6 Hz, 2H, CH); MS *m/z* 1123.5973 ($C_{60}H_{87}N_2O_{18}^+$ calculated 1123.5948). Dye **7b** (62.7 mg, 58 μmol) was reacted according to the procedure described above and produced 44 mg (66%) of dye **8b**. ^{1}H NMR (400 MHz, MeOD-d_6): δ 1.30 (t, *J* = 8 Hz, 4H, CH_2), 1.48 (t, *J* = 8 Hz, 4H, CH_2), 1.63 (t, *J* = 8 Hz, 4H, CH_2), 1.78 (s, 12H, CH_3), 2.55 (t, *J* = 8 Hz, 2H, CH_2), 3.05 (t, *J* = 8 Hz, 2H, CH_2), 3.44−3.61 (m, 34H, CH_2), 3.78 (t, *J* = 8 Hz, 4H, CH), 5.81 (d, *J* = 12 Hz, 2H, CH), 7.21−7.27 (m, 6H, CH_{ar}), 7.40 (t, *J* = 8 Hz, 2H, CH_{ar}), 7.5 (t, 4H, *J* = 8 Hz, 4H, CH_{ar}), 8.34 (d, *J* = 12 Hz, 2H, CH); MS *m/z* 1123.5973 ($C_{60}H_{87}N_2O_{18}^+$ calculated 1123.5948).

Dye **7c** (25 mg, 23 μmol) was reacted according to the procedure described above affording 20.3 mg (76%) of dye **8c**. ^{1}H NMR (400 MHz, MeOD-d_6): δ 1.74 (s, 12H, CH_3), 2.52 (t, *J* = 7.8 Hz, 2H, CH_2), 2.98 (t, *J* = 7.6 Hz, 2H, CH_2), 3.33−3.71 (m, 42H, CH_2), 3.96 (s, 4H, CH), 5.89 (d, *J* = 14 Hz, 2H, CH), 7.18−7.25 (m, 6H, CH_{ar}), 7.33 (t, *J* = 8 Hz, 2H, CH_{ar}), 7.43 (t, *J* = 8 Hz, 4H, CH_{ar}), 8.27 (d, *J* = 14.4 Hz, 2H, CH); MS *m/z* 1123.5973 ($C_{60}H_{87}N_2O_{18}^+$ calculated 1123.5948). To a solution of dye **7d** (223 mg, 0.15 mmol) in vented water (4.5 mL) was added 4-(2-carboxyethyl)benzeneboronic acid (70 mg, 0.28 mmol) and $PdCl_2$ (dppf) (26 mg, 0.03 mmol) and the mixture was stirred at 70 °C overnight. The solvent was removed in vacuum and the residue was purified by automated flash chromatography using dichlormethane/methanol (0−80% methanol) and RP-C18 flash chromatography using water/methanol (0−50% methanol) to afford 72.8 mg (31%) of dye **8d** as a blue solid. ^{1}H NMR (400 MHz, MeOD-d_6): δ 1.78 (s, 12H, CH_3), 2.71 (t, *J* = 8 Hz, 2H, CH_2), 3.04 (t, *J* = 8 Hz, 2H, CH_2), 3.44−3.63 (m, 86H, CH_2, CH_3), 3.69 (t, 4 Hz, CH_2), 4.00 (t, 4H, CH), 5.92 (d, *J* = 16 Hz, 2H, CH), 7.26 (t, *J* = 8 Hz, 6 H, CH_{ar}), 7.38 (t, *J* = 8 Hz, 2 H, CH_{ar}), 7.46−7.51 (m, 4H, CH_{ar}), 8.32 (d, *J* = 16 Hz, 2H, CH); MS *m/z* 1499.8882 ($C_{80}H_{127}N_2O_{24}^+$ calculated 1499.8773).

Preparation of NHS Esters ***9***. A mixture of dye **8** (4.67 μmol), HSTU (14 μmol), and DIPEA (14 μmol) in DMF (185 μL) was stirred at rt for 2 d and precipitated in diethyl ether, isolated by filtration, and dried in vacuum. Dye **8a** (5 mg, 4.67 μmol) was reacted according to the above-described procedure to afford 4.6 mg (84%) of dye **9a**. MS *m/z* 1132.5548 ($C_{60}H_{82}N_3O_{18}^+$ calculated 1132.5588). Dye **8b** (6.3 mg, 5.4 μmol) was reacted according to the procedure described above and yielded 6 mg (88%) of dye **9b**. MS *m/z* 1217.6542 ($C_{66}H_{94}N_3O_{18}^+$ calculated 1217.6527). Dye **8c** (5 mg, 4.3 μmol) was reacted according to the above-described procedure to obtain 4.5 mg (83%) of dye **9c**. MS *m/z* 1220.6075 $C_{64}H_{90}N_3O_{20}^+$ calculated 1220.6112). Dye **8d** (7.8 mg, 4.8 μmol) was reacted according to the procedure described above and produced 8.6 mg (91%) of dye **9d**. MS *m/z* 1596.8961 ($C_{84}H_{130}N_3O_{26}^+$ calculated 1596.8937). Dye **8e** (5 mg, 6.27 μmol) was reacted according to the above-described procedure which gave 5.9 mg (93%) of dye **9e**. MS *m/z* 916.2846 ($C_{46}H_{52}N_3Na_2O_{10}S_2^+$ calculated 916.2884).

DOI: 10.1021/acs.bioconjchem.5b00097
Bioconjugate Chem. 2015, 26, 773−781

Preparation of Cetuximab Conjugates. Cetuximab (5 mg, 33 μmol) was dissolved in 750 μL of PBS (pH 7.4), which was followed by addition of a solution of dye NHS ester **9a−e** from a stock solution of the respective dye in PBS (1.3−3 mg/mL). The ratio of cetuximab and the reactive dye used in molar excess was within 2−20 mol equiv. The reaction mixtures were gently shaken overnight at room temperature. Purification was performed with Sephadex columns (NAP25, Amersham) and PBS as eluent. The absence of unbound dye in the conjugate solutions was confirmed by thin layer chromatography (RP-C18 TLC). The resulting solutions of the dye−cetuximab conjugates **10b−e** were then analyzed with respect to their dye-to-protein (D/P) ratio. D/P values were determined using the integral method.[29] The concentration of the attached dye was determined by employing the integral absorption coefficient in contrast to the molar absorption coefficient at the maximum of the absorption signal of the dye.[30,31] This procedure gives more correct values, because the method is independent from dye dimerization processes. The molar extinction coefficient of cetuximab (174 000 $L \cdot mol^{-1}$ cm^{-1}) was taken from the literature.[32,33]

Cell Studies. Cell studies were conducted with human lung cancer cell line A431 that expressed the EGF receptor and a low-EGF receptor expressing human epidermoid cell line A549. Cells were propagated with DENEM medium, with 10% fetal calf serum (FCS), 2% glutamine, and penicillin/streptomycin (PAN Biotech) and seeded into the medium at 1×10^5 cells/mL, cultured at 37 °C with 5% CO_2, and split 1:5 two times a week. In the present study, A549 or A431 cells were seeded on a 5×10^4 cells/mL in a 24-well culture plate on glass coverslips (Sigma) and cultured for 24 h at 37 °C. Subsequently, the cells were incubated at 37 °C with the medium for 1 h with 5 μg/mL of antibody test substances. Afterward the cells were fixed with cold acetone and rinsed. 4,6-Diamino-2-phenylindole (DAPI, Abcam) was used for nuclear counterstain. Images were obtained from a confocal microscope (Zeiss LSM 5 Exciter).

■ ASSOCIATED CONTENT

Supporting Information

^{1}H NMR spectra and HPLC data of dyes **8a−d**. This material is available free of charge via the Internet at http://pubs.acs.org.

■ AUTHOR INFORMATION

Corresponding Author

*E-mail: licha@mivenion.com. Phone: ++49 30 688379230. Fax: ++49 30 688379299.

Notes

The authors declare no competing financial interest.

■ ACKNOWLEDGMENTS

This work was funded in part by Dahlem Research School. The author would like to thank Ms. Nicole Wegner, Ms. Sylvia Kern, and Mr. Ingo Steinke for their technical assistance.

■ REFERENCES

(1) Licha, K., and Resch-Genger, U. (2011) Probes for optical imaging: new developments. *Drug Discovery Today: Technol. 8*, 87−94.

(2) Yuan, L., Lin, W., Zheng, K., He, L., and Huang, W. (2013) Far-red to near infrared analyte-responsive fluorescent probes based on organic fluorophore platforms for fluorescence imaging. *Chem. Soc. Rev. 42*, 622−661.

(3) Steiger, R., Pugin, R., and Heier, J. (2009) J-aggregation of cyanine dyes by self-assembly. *Colloids Surf., B 74*, 484−491.

(4) Lanzafame, J. M., Min, L., Miller, R. J. D., Muenter, A. A., and Parkinson, B. A. (1991) Electron injection from adsorbed oxazine into SnS. *Mol. Cryst. Liq. Cryst. 194*, 287.

(5) Möbius, D. (1995) Scheibe aggregates. *Adv. Mater. 7*, 437.

(6) Tyutyulkov, N., Fabian, J., Mehlhorn, A., Dietz, F., and Tadjer, A. (1991) *Polymethine Dyes: Structure and Properties*, Kliment Ohridski University Press, Sofia.

(7) Tani, T. (1995) Photographic Sensitivity: Theory and Mechanisms. In *Oxford Series on Optical and Imaging Sciences*, p 111, Chapter 5, Oxford University Press, New York.

(8) Arden, J., Deltau, G., Huth, V., Kringel, U., Peros, D., and Drexhage, K. H. (1991) Fluorescence and lasing properties of rhodamine dyes. *J. Lumin. 49*, 352.

(9) Licha, K., and Olbrich, C. (2005) Optical imaging in drug discovery and diagnostic applications. *Adv. Drug Delivery Rev. 57*, 1087−1108.

(10) Jelly, E. E. (1936) Spectral absorption and fluorescence of dyes in the molecular state. *Nature 138*, 1009.

(11) Würthner, F., Kaiser, T. E., and Saha-Müller, C. R. (2011) J-Aggregates: from serendipitous discovery to supramolecular engineering of functional dye materials. *Angew. Chem., Int. Ed. 50*, 3376−3410.

(12) Kumar, V., Baker, G. A., and Pandey, S. (2011) Ionic liquid-controlled J- versus H-aggregation of cyanine dyes. *Chem. Commun. 47*, 4730−4732.

(13) Licha, K. (2002) Contrast Agents for Optical Imaging. In *Topics in Current Chemistry*, Contrast Agents II, pp 1−29, Vol *222*, Springer, Heidelberg.

(14) Renikuntla, B. R., Rose, H. C., Eldo, J., Waggoner, A. S., and Armitage, B. A. (2004) Improved photostability and fluorescence properties through polyfluorination of a cyanine dye. *Org. Lett. 6*, 909−912.

(15) Heek, T., Fasting, C., Rest, C., Zhang, X., Würthner, F., and Haag, R. (2010) Highly fluorescent water-soluble polyglycerol-dendronized perylene bisimide dyes. *Chem. Commun. 46*, 1884−1886.

(16) Yang, S. K., Shi, X., Park, S., Doganay, S., Ha, T., and Zimmerman, S. C. (2011) *J. Am. Chem. Soc. 133*, 9964−9967.

(17) Heek, T., Nikolaus, J., Schwarzer, R., Fasting, C., Welker, P., Licha, K., Herrmann, A., and Haag, R. (2013) An amphiphilic perylene imido diester for selective cellular imaging. *Bioconjugate Chem. 24*, 153−158.

(18) Zill, A. T., Licha, K., Haag, R., and Zimmerman, S. C. (2012) Synthesis and properties of fluorescent dyes conjugated to hyperbranched polyglycerols. *New J. Chem. 36*, 419−427.

(19) Wyszogrodzka, M., Möws, K., Kamlage, S., Wodzińska, J. R., Plietker, B., and Haag, R. (2008) New approaches towards monoamino polyglycerol dendrons and dendritic triblock amphiphiles. *Eur. J. Org. Chem.*, 53−63.

(20) Wyszogrodzka, M., and Haag, R. (2009) Synthesis and characterization of glycerol dendrons, self-assembled monolayers on gold: a detailed study of their protein resistance. *Biomacromolecules 10*, 1043−1054.

(21) Kiyose, K., Hanaoka, K., Oushiki, D., Nakamura, T., Kajimura, M., Suematsu, M., Nishimatsu, H., Yamane, T., Terai, T., Hirata, Y., et al. (2010) Hypoxia-sensitive fluorescent probes for in vivo real-time fluorescence imaging of acute ischemia. *J. Am. Chem. Soc. 132* (45), 15846−15848.

(22) Harris, J. M., Struck, E. C., Case, M. G., Paley, M. S., Yalpani, M., Van Alstine, J. M., and Brooks, D. E. (1984) Synthesis and characterization of poly(ethylene glycol) derivatives. *J. Polym. Sci., Polym. Chem. Ed. 22*, 341−352.

(23) Owens, E. A., Hyun, H., Kim, S. H., Lee, J. H., Park, G., Ashitate, Y., Choi, J., Hong, G. H., Alyabyev, S., Lee, et al. (2013) Highly charged cyanine fluorophores for trafficking scaffold degradation. *Biomed. Mater. 8*, 014109.

(24) Hirata, T., Kogiso, H., Morimoto, K., Miyamoto, S., Taue, H., Sano, S., Muguruma, N., Ito, S., and Nagao, Y. (1998) Synthesis and reactivities of 3-indocyanine-green-acyl-1,3-thiazolidine-2-thione (ICG-ATT) as a new near-infrared fluorescent-labeling reagent. *Bioorg. Med. Chem. 6*, 2179−2184.

DOI: 10.1021/acs.bioconjchem.5b00097
Bioconjugate Chem. 2015, 26, 773−781

(25) Lee, H., Mason, J. C., and Achilefu, S. (2008) Synthesis and spectral properties of near-infrared aminophenyl-, hydroxyphenyl-, and phenyl-substituted heptamethine cyanines. *J. Org. Chem. 73*, 723−725.
(26) Pauli, J., Licha, K., Berkemeyer, J., Grabolle, M., Spieles, M., Wegner, N., Welker, P., and Resch-Genger, U. (2013) New fluorescent labels with tunable hydrophilicity for the rational design of bright optical probes for molecular imaging. *Bioconjugate Chem. 24*, 1174−1185.
(27) Weinhart, M., Grunwald, I., Wyszogrodzka, M., Gaetjen, L., Hartwig, A., and Haag, R. (2010) Linear poly(methyl glycerol and linear polyglycerol as potent protein and cell resistant alternatives to poly(ethylene glycol). *Chem.—Asian J. 5* (9), 1992−2000.
(28) Grabolle, M., Pauli, J., and Resch-Genger, U. (2014) Structural control of dye−protein binding, aggregation and hydrophilicity in a series of asymmetric cyanines. *Dyes Pigm. 103*, 118−126.
(29) Grabolle, M., Brehm, R., Pauli, J., Dees, F. M., Hilger, I., and Resch-Genger, U. (2012) Determination of the labeling density of fluorophore−biomolecule conjugates with absorption spectroscopy. *Bioconjugate Chem. 23* (2), 287−292.
(30) Mujumdar, R. B., Ernst, L. A., Mujumdar, S. R., Lewis, C. J., and Waggoner, A. S. (1993) Cyanine dye labeling reagents: Sulfoindocyanine succinimidyl esters. *Bioconjugate Chem. 4*, 105.
(31) Haughland, R. P (1995) Coupling of monoclonal antibodies with fluorophores. In *Methods in Molecular Biology*, pp 205−221, Vol *45*, Humana Press, Totowa, NJ.
(32) http://www.drugbank.ca.
(33) http://web.expasy.org/protparam/.

DOI: 10.1021/acs.bioconjchem.5b00097
Bioconjugate Chem. 2015, 26, 773−781